



Optics Letters

Vector partially coherent beams with prescribed non-uniform correlation structure

JIAYI YU,¹ XINLEI ZHU,² SHUQIN LIN,¹ FEI WANG,^{2,4} GREG GBUR,^{3,5}  AND YANGJIAN CAI^{1,2,6}

¹Shandong Provincial Engineering and Technical Center of Light Manipulations and Shandong Provincial Key Laboratory of Optics and Photonic Device, School of Physics and Electronics, Shandong Normal University, Jinan 250014, China

²School of Physical Science and Technology, Soochow University, Suzhou 215006, China

³Department of Physics and Optical Science, University of North Carolina at Charlotte, Charlotte, North Carolina 28223, USA

⁴e-mail: fwang@suda.edu.cn

⁵e-mail: gjgbur@uncc.edu

⁶e-mail: yangjiancai@suda.edu.cn

Received 11 May 2020; revised 5 June 2020; accepted 6 June 2020; posted 8 June 2020 (Doc. ID 397316); published 1 July 2020

We introduce a general strategy for the synthesis of vector partially coherent beams (PCBs) with a prescribed non-uniform correlation structure. With it, we characterize a specific family of such beams, termed radially polarized Hermite non-uniformly correlated (RPHNUC) beams. These beams possess unusual propagation properties compared to vector PCBs with uniform correlation structure; for example, they maintain their dark hollow core and evolve multi-ring structures. These beams may prove useful in free-space optical communications, optical trapping, and polarization-sensitive imaging. © 2020 Optical Society of America

<https://doi.org/10.1364/OL.397316>

Although polarization is a fundamental property of light fields, researchers have only recently investigated how non-trivial polarization states can be used to produce novel optical effects. Traditionally, most studies have focused on beams with a spatially uniform state of polarization (SOP), but it is now appreciated that beams with a non-uniform SOP (e.g., radially or azimuthally polarized beams) [1] are advantageous in many applications. For example, radially polarized beams have been shown to have a smaller focal spot [2], and non-uniformly polarized beams have been shown to have improved resistance to atmospheric turbulence [3]. Vector beams are now a vibrant and active topic of research.

Spatial coherence is also an important property of laser beams, and beams with decreased spatial coherence, called partially coherent beams (PCBs), often have advantages over their coherent counterparts [4,5]. In 2007, a powerful new method for designing correlation functions of scalar PCBs was introduced by Gori *et al.* [6], allowing a wide variety of novel PCBs to be investigated [4,5]. One broad and extremely important class derived from the formalism by Gori *et al.* is non-uniformly correlated beams [7], which possess a non-homogeneous degree of coherence. Such beams display many potentially beneficial properties on propagation, such as improved resistance to atmospheric turbulence [8,9].

The combination of polarization and partial coherence has led to the discovery of novel effects. It was long assumed that the SOP and the degree of polarization (DOP) of vector beams remain invariant on propagation in free space. In 1994, however, James predicted that the DOP of PCBs can change on propagation [10]; this was subsequently verified experimentally by Vidal *et al.* [11]. Wolf introduced a unified theory of polarization and coherence in 2003, allowing for the systematic study of vector PCBs [12]. Using this, it was shown by Korotkova and Wolf [13] that the SOP of stochastic electromagnetic beams may change on propagation as well. In 2008, Salem and Wolf explored the phenomenon of coherence-induced polarization changes in detail and predicted that the polarization properties of vector beams could be modulated by varying their spatial coherence width [14]. These studies as a whole demonstrated that coherence and polarization are closely connected and that much can be learned from their synthesis.

In 2009, Gori *et al.* extended their method for designing correlation functions from scalar to electromagnetic waves [15], allowing the development of many new classes of vector PCBs. Since then, researchers have investigated the different behaviors of vector PCBs arising due to different coherence structures [16,17]. However, a vast majority of these works have focused on uniformly correlated (or Schell-model) sources, and only a few papers have studied vector PCBs with a non-uniformly correlated structure. It is expected that, just as non-uniformly polarized and non-uniformly correlated beams have shown advantages separately in optical applications, their combination will allow even greater improvements.

In this Letter, we introduce a general strategy for the synthesis of vector PCBs with a prescribed non-uniform coherence and we employ it to generate radially polarized PCBs with Hermite non-uniform correlation (RPHNUC) beams, and we examine their free-space propagation. These beams possess propagation characteristics very different from radially polarized partially coherent (RPPC) beams (which possess uniform coherence at the source).

Typically, the spatial coherence properties of vector PCBs are characterized by either the beam coherence-polarization

matrix in the space–time domain [18] or the cross-spectral density (CSD) matrix in the space–frequency domain [19]. In recent years, the CSD matrix has become the quantity of choice for researching broadband fields. The CSD matrix of quasi-monochromatic fields at two position vectors \mathbf{r}_1 and \mathbf{r}_2 at the source plane is defined as

$$\overset{\leftrightarrow}{\mathbf{W}}(\mathbf{r}_1, \mathbf{r}_2) = \begin{bmatrix} W_{xx}(\mathbf{r}_1, \mathbf{r}_2) & W_{xy}(\mathbf{r}_1, \mathbf{r}_2) \\ W_{yx}(\mathbf{r}_1, \mathbf{r}_2) & W_{yy}(\mathbf{r}_1, \mathbf{r}_2) \end{bmatrix}, \quad (1)$$

with elements

$$W_{\alpha\beta}(\mathbf{r}_1, \mathbf{r}_2) = \langle E_{\alpha}^*(\mathbf{r}_1) E_{\beta}(\mathbf{r}_2) \rangle, \quad (\alpha, \beta = x, y). \quad (2)$$

The quantities E_x and E_y in Eq. (2) denote two mutually orthogonal components of the random electric field vector along the x and y directions, respectively, which are perpendicular to the z axis. The asterisk denotes the complex conjugate, and the angular brackets denote an average over a monochromatic ensemble. Though the CSD matrix is dependent on frequency ω , we will work at a single frequency and suppress its explicit depiction.

From the result of Gori *et al.* [15], it is known that any CSD matrix expressed in the following one-dimensional integral form is physically realizable:

$$W_{\alpha\beta}(\mathbf{r}_1, \mathbf{r}_2) = \int p_{\alpha\beta}(v) V_{\alpha}^*(\mathbf{r}_1, v) V_{\beta}(\mathbf{r}_2, v) dv, \quad (3)$$

where $p_{\alpha\beta}(v)$ are the elements of the following weighting matrix:

$$\overset{\leftrightarrow}{p}(v) = \begin{bmatrix} p_{xx}(v) & p_{xy}(v) \\ p_{xy}^*(v) & p_{yy}(v) \end{bmatrix}, \quad (4)$$

and the elements of the weighting matrix must satisfy the following inequalities:

$$p_{xx}(v) \geq 0, \quad p_{yy}(v) \geq 0, \quad p_{xx}(v)p_{yy}(v) \geq |p_{xy}(v)|^2. \quad (5)$$

We take $V_{\alpha(\beta)}(\mathbf{r}, v)$ to be a kernel of the form

$$V_{\alpha(\beta)}(\mathbf{r}, v) = \tau_{\alpha(\beta)}(\mathbf{r}) \exp[-ik\mathcal{R}(\mathbf{r})v], \quad (6)$$

where k is the wavenumber, $\tau_{\alpha(\beta)}(\mathbf{r})$ is a complex scalar function of coordinate \mathbf{r} , and $\mathcal{R}(\mathbf{r})$ is a real scalar function of coordinate \mathbf{r} .

Substituting from Eqs. (4) and (6) into Eq. (3), we obtain the expression

$$W_{\alpha\beta}(\mathbf{r}_1, \mathbf{r}_2) = \tau_{\alpha}^*(\mathbf{r}_1) \tau_{\beta}(\mathbf{r}_2) \mu_{\alpha\beta}(\mathbf{r}_1, \mathbf{r}_2), \quad (7)$$

where $\tau_{\alpha(\beta)}(\mathbf{r})$ represents the average $\alpha(\beta)$ th component of the electric field, and $\mu_{\alpha\beta}(\mathbf{r}_1, \mathbf{r}_2)$ is the Fourier transform of $p_{\alpha\beta}(v)$, i.e.,

$$\mu_{\alpha\beta}(\mathbf{r}_1, \mathbf{r}_2) = \tilde{p}_{\alpha\beta}[\mathcal{R}(\mathbf{r}_2) - \mathcal{R}(\mathbf{r}_1)]. \quad (8)$$

The SOP of the vector PCB is closely related to $\tau_{\alpha}(\mathbf{r})$. For example, if we set $\tau_{\alpha}(\mathbf{r}) = A_{\alpha} \exp(-\frac{\mathbf{r}^2}{4w_0^2})$, with A_{α} being a constant and w_0 being the beam width, the beam exhibits a uniform SOP: the SOP at any point in the source plane is the same. Such beams are referred to as uniformly polarized PCBs. In contrast, if we set

$$\tau_{\alpha}(\mathbf{r}) = \frac{\alpha}{2w_0} \exp\left(-\frac{\mathbf{r}^2}{4w_0^2}\right), \quad (9)$$

the beam exhibits a non-uniform radial SOP and is a radially polarized PCB. We may also choose $\tau_x(\mathbf{r}) = \frac{y}{2w_0} \exp(-\frac{\mathbf{r}^2}{4w_0^2})$ and $\tau_y(\mathbf{r}) = \frac{x}{2w_0} \exp(-\frac{\mathbf{r}^2}{4w_0^2})$, in which case, we have an azimuthally polarized PCB.

The correlation structure of a PCB depends on the choices for $p_{\alpha\beta}(v)$ and $\mathcal{R}(\mathbf{r})$. If we take $p_{\alpha\beta}(v)$ of Gaussian form and $\mathcal{R}(\mathbf{r})$ linear in the coordinate \mathbf{r} , PCBs with a pseudo-Schell-model structure are generated [20]; if $p_{\alpha\beta}(v)$ has a non-Gaussian form and $\mathcal{R}(\mathbf{r})$ is not linear in \mathbf{r} , the result is a PCB with a non-uniform correlation structure.

With different choices of $\tau_{\alpha(\beta)}(\mathbf{r})$, $p_{\alpha\beta}(v)$, and $\mathcal{R}(\mathbf{r})$, we can generate a variety of vector PCBs with distinct non-uniform correlations.

In order to demonstrate the extraordinary properties of vector PCBs with a prescribed non-uniform correlation structure, we now focus on the particular example of RPHNUC beams. We introduce a source with $\tau_{\alpha}(\mathbf{r})$ in the radially polarized form given in Eq. (9), and take $p_{\alpha\beta}(v)$ to have the form

$$p_{\alpha\beta}(v) = B_{\alpha\beta} (2v/a_{\alpha\beta})^{2m} \exp(-v^2/a_{\alpha\beta}^2) / (\sqrt{\pi} a_{\alpha\beta}), \quad (10)$$

with constraints on $a_{\alpha\beta}$ and $B_{\alpha\beta}$ to be determined.

We further take $\mathcal{R}(\mathbf{r}) = \mathbf{r}^2$. Then, according to Eq. (8), we obtain

$$\mu_{\alpha\beta}(\mathbf{r}_1, \mathbf{r}_2) = G_0 B_{\alpha\beta} \exp\left[-\frac{(\mathbf{r}_1^2 - \mathbf{r}_2^2)^2}{r_{\alpha\beta}^4}\right] H_{2m}\left(\frac{\mathbf{r}_1^2 - \mathbf{r}_2^2}{r_{\alpha\beta}^2}\right), \quad (11)$$

where $r_{\alpha\beta}^2 \equiv 2/ka_{\alpha\beta}$ is the coherence length, $H_{2m}(x)$ denotes the Hermite polynomial of order $2m$, $G_0 = 1/H_{2m}(0)$, and $B_{\alpha\beta} = |B_{\alpha\beta}| \exp(i\phi_{\alpha\beta})$ is the maximum correlation between the E_{α} and E_{β} field components. Equation (11) shows that the beam is radially polarized and has a non-uniform correlation of Hermite function form, and we have consequently labeled this beams as RPHNUC beams.

For the remainder of this Letter, we focus primarily on RPHNUC beams. First, we determine the conditions that RPHNUC beams must satisfy to be a realizable correlation function. These beams must meet the following three conditions: a) the CSD matrix must be quasi-Hermitian [15], i.e., $W_{\alpha\beta}(\mathbf{r}_1, \mathbf{r}_2) = W_{\beta\alpha}^*(\mathbf{r}_2, \mathbf{r}_1)$; b) the beams must satisfy the nonnegative conditions given in Eq. (5); and c) the radial polarization condition must be met: in the source plane, the field is linearly polarized, and the polarization orientation angle at any point should satisfy $\theta(x, y) = \arctan(y/x)$ [21]. The SOP of the beams can be characterized with the polarization ellipse, whose orientation angle θ and degree of ellipticity ε are expressed as Eqs. (A3) and (A4) in Ref. [21]. In order to satisfy the above conditions, our RPHNUC beams must additionally satisfy

$$B_{xy} = B_{yx} = 1, \quad r_{xx} = r_{yy} = r_{yx} = r_c, \quad (12)$$

where r_c is the correlation length.

Paraxial propagation of the CSD of a PCB through a stigmatic $ABCD$ optical system can be described by the generalized Collins formula [22]

$$\begin{aligned}
& W_{\alpha\beta}(\rho_1, \rho_2, z) \\
&= \frac{1}{(\lambda B)^2} \exp\left[-\frac{ikD}{2B}(\rho_1^2 - \rho_2^2)\right] \iint_{-\infty}^{\infty} W_{\alpha\beta}(\mathbf{r}_1, \mathbf{r}_2) \\
&\quad \times \exp\left[\frac{ik}{B}(\mathbf{r}_1 \cdot \rho_1 - \mathbf{r}_2 \cdot \rho_2) - \frac{ikA}{2B}(\mathbf{r}_1^2 - \mathbf{r}_2^2)\right] d^2\mathbf{r}_1 d^2\mathbf{r}_2, \quad (13)
\end{aligned}$$

where $\rho_1 \equiv (\rho_{1x}, \rho_{1y})$ and $\rho_2 \equiv (\rho_{2x}, \rho_{2y})$ are two arbitrary transverse position vectors in the output plane; A, B, C, D are the elements of the transfer matrix for the stigmatic optical system.

We may calculate the CSD of RPHNUC beams in the target plane using the above equations. By substituting from Eqs. (3), (6), and (10) into Eq. (13), and interchanging the order of integration, we obtain the formula

$$W_{\alpha\beta}(\rho_1, \rho_2, z) = \int p_{\alpha\beta}(v) P_{\alpha\beta}(\rho_1, \rho_2, v) dv, \quad (14)$$

where we have obtained

$$\begin{aligned}
P_{\alpha\beta}(\rho_1, \rho_2, v) &= \frac{k^2 \rho_{1\alpha} \rho_{2\beta}}{64 B^4 w_0^2 |\xi|^4} \exp\left[-\frac{ikD}{2B}(\rho_1^2 - \rho_2^2)\right] \\
&\quad \times \exp\left(-\frac{k^2}{4B^2 \xi} \rho_1^2 - \frac{k^2}{4B^2 \xi^*} \rho_2^2\right), \quad (15)
\end{aligned}$$

with $\xi = \frac{1}{4w_0^2} - ik(v - \frac{A}{2B})$. Hence, we have obtained the CSD matrix of RPHNUC beams in the output plane after propagation by evaluating Eqs. (14) and (15).

Two quantities are of particular interest in beam propagation. The spectral intensity $S(\rho)$ of the beam in a given plane, usually the output plane of the optical system, is defined as

$$S(\rho) = \text{Tr} \vec{\mathbf{W}}(\rho_1, \rho_2) = W_{xx}(\rho, \rho) + W_{yy}(\rho, \rho). \quad (16)$$

The DOP in the output plane is given by the expression

$$P(\rho) = \sqrt{1 - 4 \text{Det}[\vec{\mathbf{W}}(\rho, \rho)] / \{\text{Tr}[\vec{\mathbf{W}}(\rho, \rho)]\}^2}. \quad (17)$$

Using the expressions we derived above, we next study the propagation properties of RPHNUC beams in free space. The transfer matrix for free-space propagation over distance z is $A = 1; B = z; C = 0; D = 1$. In the following calculations, we choose the beam parameters as $\lambda = 632.8$ nm, $w_0 = 1$ cm, $r_c = 0.6$ cm. The correlation length r_c is less than the beam width w_0 , but significantly larger than the wavelength; the result is a partially coherent field that retains beam-like directionality.

We begin by comparing the evolution of the intensity of RPHNUC beams with conventional RPPC beams, which possess a Schell-model correlation structure. Figure 1(a) shows the evolution of the RPPC beam on propagation, which was studied in detail in Ref. [21]. It can be seen that although the RPPC beam begins with a dark hollow core in the source plane, this dark core becomes shallower on propagation and eventually degrades to a Gaussian intensity profile. This in turn indirectly indicates that the radial polarization structure is lost on propagation, as we will later see.

In contrast, Figs. 1(b) and 1(c) show the evolution of RPHNUC beams for two different beam orders, $m = 0$ and

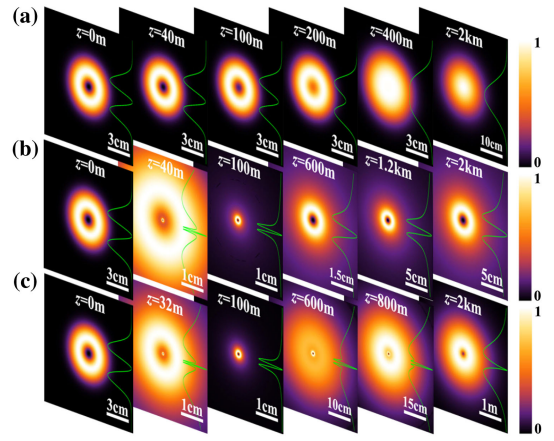


Fig. 1. Density plot of the normalized intensity of (a) RPPC beam and RPHNUC beams upon propagation in free space at different distances with different beam orders (b) $m = 0$ and (c) $m = 1$.

$m = 1$. In both cases, it can be seen that the RPHNUC beams evolve in a non-trivial manner, manifesting rings of different sizes, sometimes multiple rings, at different intermediate distances. However, the dark hollow core of the beam is always maintained, even after propagating several kilometers. Over short propagation distances, notably in the second and third images in Figs. 1(b) and 1(c), a new ring manifests in the center of the beam with an extremely small radius. It is to be noted that the transverse scales of the figures have been changed to highlight this feature. This small ring grows in size and intensity on propagation, while the outside ring diminishes and disappears.

RPHNUC beams also exhibit self-focusing properties typical of a non-uniformly correlated source. Figure 2(a) shows the ratio of the maximum intensity in a plane of constant z to the maximum intensity in the source plane for RPPC beams and RPHNUC beams of different orders. The most noticeable feature in the plot is the sharp increase in maximum intensity for RPHNUC beams, indicative of self-focusing; this feature is not present for the RPPC beam. This self-focusing becomes more dramatic as the beam order is increased, which is consistent with the results for scalar HNUC beams [9,23]. Over longer distances, the maximum intensity decreases, consistent with normal diffractive spreading. Over short propagation distances, as shown in the inset in Fig. 2(a), the maximum intensity first increases, then decreases; we interpret this as arising from the interplay between the intensities of the outer ring and inner ring.

We have noted that RPHNUC beams appear to maintain their dark hollow core on propagation; this is quantified in

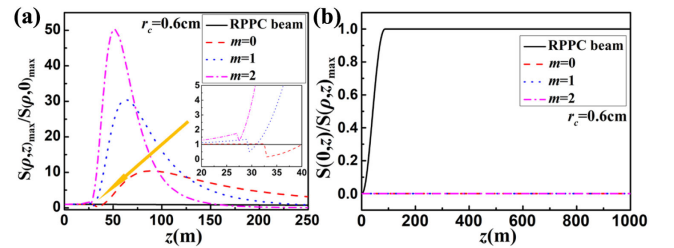


Fig. 2. Ratio of (a) maximum intensity in the transverse plane $S_{\max}(\rho, z)$ to that in the source plane $S_{\max}(\rho, 0)$ and (b) on-axis intensity $S(0, z)$ to the maximum intensity $S_{\max}(\rho, z)$ for different beam orders.

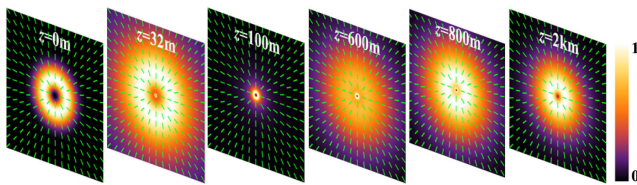


Fig. 3. Density plot of the normalized intensity and the SOP of RPHNUC beams ($m = 1$) upon propagation in free space at different distances.

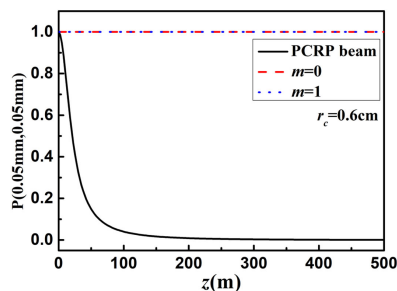


Fig. 4. DOP of RPPC and RPHNUC beams at point (0.5 mm, 0.5 mm) versus the propagation distance z for different beam orders.

Fig. 2(b), in which the ratio of the on-axis intensity to the maximum intensity in a plane of constant z is plotted. For the RPPC beam, the ratio quickly goes to unity, indicating that the hollow core quickly becomes a maximum of intensity; for RPHNUC beams, the ratio remains zero, indicating that the dark hollow core is maintained at all propagation distances.

The polarization properties of RPHNUC beams are also maintained on propagation. Figure 3 again shows the intensity of a RPHNUC beam with $m = 1$ for different propagation distances. Both these figures, and the overlaid vector plot of the SOP, show that the beam maintains radial polarization over all propagation distances. This evolution is dramatically different from the behavior of RPPC beams, which depolarize on propagation (see Fig. 1 in Ref. [24]). Figure 4 shows the DOP at the particular point (0.05 mm, 0.05 mm) versus propagation distance z for different beam types and orders. The RPPC beam becomes unpolarized as it propagates, as has been previously noted [21], while the RPHNUC beams remain fully polarized. With RPHNUC beams, then, we have a class of partially coherent beams that maintain both their DOP and SOP at any propagation distance in free space.

We may explain these unique beam propagation features by viewing Eq. (3) as an integral over coherent modes of the beam [9]. Equation (6) shows that each of the modes possesses a quadratic phase factor, $\exp(-ikvr^2)$, which causes them to individually converge at different focal distances given by the expression $z = 1/2v$. At different propagation distances, then, different modes will dominate. Furthermore, each mode possesses a dark hollow core, and modes are only focused/defocused and not shifted; they all maintain their dark core on propagation. Therefore RPHNUC beams maintain their dark hollow core and radial polarization and remain fully polarized over long propagation distances. Conventional RPPC beams, in contrast, may be interpreted as being created by random tilts of a radially polarized beam. The dark core of the beam “wanders” in the ensemble, and on average will not persist on propagation.

In this Letter, we have therefore introduced a general method for constructing vector PCBs and shown in particular that RPHNUC beams display unique features on propagation that are distinct from conventional RPPC beams with a uniform correlation structure. In practice, these beams could be synthesized by using a pseudo-mode sampling superposition method [25], weighting them as in Eq. (3).

These beams may prove useful for a number of applications. Their robustness may allow them to be used as information carriers in free-space optical communication, where they possess the benefits of non-uniform polarization and partial coherence. Their self-focusing and polarization characteristics may prove useful in optical trapping, where the strength and position of the trap can be adjusted through the coherence properties. Finally, the existence of fine structure in space and polarization may allow them to be used in polarization-sensitive imaging schemes.

Funding. National Key Research and Development Program of China (2019YFA0705000); National Natural Science Foundation of China (11525418, 11874046, 11947240, 11974218, 91750201); Innovation Group of Jinan (2018GXRC010).

Disclosures. The authors declare no conflicts of interest.

REFERENCES

- Q. Zhan, *Adv. Opt. Photon.* **1**, 1 (2009).
- R. Dorn, S. Quabis, and G. Leuchs, *Phys. Rev. Lett.* **91**, 233901 (2003).
- Y. Gu, O. Korotkova, and G. Gbur, *Opt. Lett.* **34**, 2261 (2009).
- Y. Cai, Y. Chen, J. Yu, X. Liu, and L. Liu, *Prog. Opt.* **62**, 157 (2017).
- Y. Cai, Y. Chen, and F. Wang, *J. Opt. Soc. Am. A* **31**, 2083 (2014).
- F. Gori and M. Santarsiero, *Opt. Lett.* **32**, 3531 (2007).
- H. Lajunen and T. Saastamoinen, *Opt. Lett.* **36**, 4104 (2011).
- Y. Gu and G. Gbur, *Opt. Lett.* **38**, 1395 (2013).
- J. Yu, F. Wang, L. Liu, Y. Cai, and G. Gbur, *Opt. Express* **26**, 16333 (2018).
- D. James, *J. Opt. Soc. Am. A* **11**, 1641 (1994).
- I. Vidal, E. J. S. Fonseca, and J. M. Hickmann, *Phys. Rev. A* **84**, 033836 (2011).
- E. Wolf, *Phys. Lett. A* **312**, 263 (2003).
- O. Korotkova and E. Wolf, *Opt. Commun.* **246**, 35 (2005).
- M. Salem and E. Wolf, *Opt. Lett.* **33**, 1180 (2008).
- F. Gori, V. Ramírez-Sánchez, M. Santarsiero, and T. Shirai, *J. Opt. A* **11**, 085706 (2009).
- Y. Chen, F. Wang, J. Yu, L. Liu, and Y. Cai, *Opt. Express* **24**, 15232 (2016).
- H. Mao, Y. Chen, C. Liang, L. Chen, Y. Cai, and S. A. Ponomarenko, *Opt. Express* **27**, 14353 (2019).
- F. Gori, *Opt. Lett.* **23**, 241 (1998).
- E. Wolf, *Introduction to the Theory of Coherence and Polarization of Light* (Cambridge University, 2007).
- J. C. G. de Sande, R. Martínez-Herrero, G. Piquero, M. Santarsiero, and F. Gori, *Opt. Express* **27**, 3963 (2019).
- G. Wu, F. Wang, and Y. Cai, *Opt. Express* **20**, 28301 (2012).
- S. A. Collins, *J. Opt. Soc. Am.* **60**, 1168 (1970).
- J. Yu, Y. Cai, and G. Gbur, *Opt. Express* **26**, 27894 (2018).
- L. Guo, Y. Chen, X. Liu, L. Liu, and Y. Cai, *Opt. Express* **24**, 13714 (2016).
- Y. Gu and G. Gbur, *J. Opt. Soc. Am. A* **27**, 2621 (2010).